

NRL REPORT NO. N-3327

FURTHER INVESTIGATIONS OF THE RADIATION FROM ROCKET MOTOR FLAMES

J. A. Curcio and J. A. Sanderson

July 26, 1948

Approved by:

E. O. Hulburt, Superintendent, Optics Division

APPROVED FOR PUBLIC
RELEASE - DISTRIBUTION
UNLIMITED



NAVAL RESEARCH LABORATORY

CAPTAIN H. A. SCHADE, USN, DIRECTOR
WASHINGTON, D.C.

DISTRIBUTION

ONR	
Attn: Code N-482	(2)
Attn: Code N-421	(3)
BuOrd	
Attn: Code Re9d	(6)
BuAer	
Attn: Code EL-71	(6)
Attn: Code TD-4	(1)
BuShips	
Attn: Code 947	(6)
Dir., USNEL	(2)
CO, USNOTS	
Attn: Reports Unit	(2)
OCSigO	
Attn: Ch. Eng. & Tech. Div., SIGTM-S	(1)
CO, SCEL	
Attn: Dir. of Eng.	(2)
CG, AMC, Wright-Patterson Air Force Base	
Attn: Aircraft Radiation Laboratory	(2)
Attn: Eng. Div., Electronics Subdiv., MCREEO-2	(1)
RDB	
Attn: Electronics Committee	(3)
Attn: Library	(2)
Attn: Navy Secretary	(1)
Science and Technology Project	
Attn: Mr. J. H. Heald	(2)

CONTENTS

Abstract	iv
Problem Status	iv
Authorization	iv
INTRODUCTION	1
SUMMARY OF RESULTS	1
Spectra of 220- and 400-Pound-Thrust Acid-Aniline Flame	1
Temperature and Emissivity	1
Total Radiation	2
Detection with Lead Sulfide System	2
Spectrum of 1000-Pound-Thrust Alcohol-Oxygen Flame	2
SPECTROSCOPY	3
Acid-Aniline Flame	3
1000-Pound-Thrust Alcohol-Oxygen Flame	5
TOTAL RADIATION INTENSITIES	6
400-Pound-Thrust Motors	6
Resumé of Radiation Measurements	7
Aerojet Results	8
ON THE DETECTION OF ACID-ANILINE ROCKETS BY LEAD SULFIDE CELLS	10
Atmospheric Transmission	10
The Spectral Intensity Viewed Through 0.082 and 7.5 cm of Water Vapor	12
Integrated Transmission Coefficients	12
Sensitive Element	16
Detection of Acid-Aniline Flames	22
CONCLUSIONS	25

ABSTRACT

The spectra of acid-aniline flames from 220- and 400-pound-thrust rocket motors were photographed in the interval 2500A to 7000A. The spectral distribution of energy was essentially that of a gray body of temperature 2712°K, emissivity 0.0055. Band systems at 3064A (NH), and at 3590A and 3883A (CN) were barely distinguishable in the continuum.

The spectrum of a 1000-pound-thrust alcohol-oxygen motor was discontinuous between 2350A and 7000A, consisting of sharp lines and band systems superposed on a weak continuum. Components of the spectrum were:

NA	5893A
CaO	5560A and 6260A
OH	2811A and 3064A
CH	4312A

The true spectral intensity of this flame was not measured.

The total radiant intensity of the acid-aniline flames was measured with a radiation thermocouple. Values of 1560 and 1800 watts/ft² steradian were obtained on separate runs of the motor. These and earlier measurements of radiant intensity were used, together with Aerojet Engineering Corporation measurements and data derived from the ultraviolet and the visible spectra of the flames, to compute detectability of rocket flames by infrared lead sulfide cell detectors. Under favorable nighttime conditions in the absence of haze, it was estimated that a 12-inch-diameter optical system with lead sulfide cell detector would exhibit signal-to-noise ratios of 50 against a 200-pound-thrust motor at horizontal range 8.8 nautical miles at 30,000 feet altitude, or 50 against a 400-pound-thrust motor at range 13 miles at 10,000 feet, or 200 against a 1000-pound-thrust motor at range 25 miles at 40,000 feet, or 9 against the same motor at range 91 miles at 20,000 feet. These estimates indicate the desirability of airborne measurements of the target strengths of rockets and jet aircraft in flight.

PROBLEM STATUS

This is an interim report on this problem.

AUTHORIZATION

NRL Problem No. N28-02 (N04-02R)

FURTHER INVESTIGATIONS OF THE RADIATION FROM ROCKET MOTOR FLAMES

INTRODUCTION

This report describes further experimental investigation of the radiation emitted by the flames from rocket motors burning nitric acid and aniline, and alcohol and oxygen, respectively. Similar measurements on acid-aniline flames were described in a previous report.¹ As in those experiments, the present measurements were made at the test stands of Reaction Motors, Inc., Dover, New Jersey, and were followed by supplementary laboratory investigations. The dates of these most recent measurements at Dover were 24 and 25 June 1947.

The aim of these experiments has been to obtain information about the spectral distribution of energy from the flames, and their temperatures and emissivities. These data are pertinent to the establishment of methods for measuring flame temperature, which is of interest in rocket-motor research, and to the determination of the target strength of rocket-powered missiles or aircraft, which is of interest in the problems of optical detection tracking and homing on such targets.

SUMMARY OF RESULTS

The results summarized below were obtained from measurements on a number of individual flames. Fuel mixtures and other operational data are not known in detail; hence, the results characterize the flames broadly but not in particular.

Spectra of 220- and 440-Pound-Thrust Acid-Aniline Flame

The spectra of the acid-aniline flames were essentially continuous between wavelengths 2500A and 7000A, but there were distinguishable weak bands at 3064A due to NH and at 3590 and 3883A due to CN. A typical spectrum is shown in Figure 1.

Temperature and Emissivity

The true spectral distribution of radiation from one acid-aniline flame was obtained by comparing the spectrum between 3600A and 6000A with the spectrum of a tungsten ribbon filament lamp operated at known temperature. Application of Wien's equation to

¹ J. A. Curcio and C. P. Butler, "Optical radiation from acid-aniline jet flames," NRL Report N-3097, April 1947

this curve led to the values:

$$\text{True temperature} = 2712^{\circ}\text{K}$$

$$\text{Emissivity} = 0.0055$$

These results are in agreement with those for similar flames given in (1). It was of interest that approximately the same small value of emissivity was obtained in both experiments, 0.006 in the first instance and 0.0055 in the second.

Total Radiation

The total radiation from uniform bright areas of two acid-aniline flames of 400-pound-thrust motors was measured with a total-radiation pyrometer consisting of a radiation thermocouple sensitive to all wavelengths between 0.2μ and 15μ and located at the focus of a concave mirror. The results indicated that the total emission of radiation in a direction at right angles to the length of the flame was 4800 to 5600 watts per square foot of flame. This measurement was made at a distance of 6 feet from the flame.

These values of total emission correspond to those of black bodies at 980°K and 1800°K . They are approximately three times greater than the value 1670 watts/ft² computed by putting the temperature 2712°K and the emissivity 0.0055, obtained spectroscopically, into the Stefan equation for total radiation. The difference may be due to higher emissivity of the flame in the region of infrared emission bands than in the visible spectrum. In the earlier experiments (see footnote 1) the direct measurement of total radiation agreed with the value computed from the measurements within the narrow band of the spectrum which was photographed.

Detection with Lead Sulfide System

These measurements of total radiation intensity and others made by the Aerojet Engineering Corporation have been used in making estimates of night detection ranges of the rocket motors with a lead sulfide cell at the focus of a 12-inch-diameter mirror. The methods of calculation and the results are given later in the report. They indicate that a signal to noise ratio of 50 might be obtained against a 220-pound motor at range 8.8 sea miles at 30,000 feet altitude, or of 50 against a 400-pound motor at 13 miles at 10,000 feet altitude, or of 9 against a 1000-pound motor at 91 miles at 20,000 feet, for examples. Detailed results will be given later in Table 4.

Spectrum of 1000-Pound-Thrust Alcohol-Oxygen Flame

The spectrum of a 1000-pound-thrust alcohol-oxygen motor was discontinuous between 2350A and 7000A. It consisted of sharp lines and bands superposed on a weak continuum. Components of the spectrum were:

Na - 5893A

CaO - 5560A and 6260A

Oh - 2811A and 3064A

CH - 4312A

The true spectral intensity of this flame was not measured.

SPECTROSCOPY

Acid-Aniline Flame

Spectra were photographed in the ultraviolet and in the visible spectral regions with a small Hilger E-31 quartz spectrograph. The diameter of the acid-aniline flame was estimated to be 6 inches. Hence, in order that the spectrograph of aperture f/12 should be completely filled with light, the distance from flame to slit could not be more than 72 inches. Therefore, the spectrograph was mounted 60 inches from the flame, turned on its side with the slit horizontal, and pointed to photograph an intense portion of the flame at about 2 feet from the orifice. A nearly neutral quartz step-wedge with steps of 3, 16, 33, 58, and 100 percent transmission was placed over the slit. The slit was 0.20 mm wide. No external optical system was used to focus the flame on the slit.

The flame was photographed on 3-1/4 x 4-1/4 inch Eastman 103-F plates. Exposure times were from 5 to 30 seconds. Mercury-arc spectra were photographed for wavelength calibration. The undeveloped plates which had been exposed to the flame spectrum were brought back to this Laboratory and spectra from a tungsten ribbon filament lamp were added, the filament being focussed on the slit with a lens in order to fill the collimator with light. The intensity of the tungsten radiation was reduced by a rotating sector of 1.56 percent transmission. The temperature of the tungsten lamp was measured with an optical pyrometer, and, in reducing densities in the flame spectrum to intensities by comparison with the tungsten spectrum, the emissivity of tungsten and the transmission of the glass envelope of the lamp were duly taken into account.

Figure 1 is a photograph of the nitric acid-aniline and the tungsten spectra taken on the same type 103-F plate. The similarity of the two spectra is apparent. The flame spectrum is seen to be continuous from wavelengths below 2500A to wavelengths above 7000A. Very weak bands at 3064A (OH), 3360A (NH), 3590A (CN) and 3883A (CN) were detected superposed on the continuous background. This continuous spectrum is probably due to incandescent carbon particles.

Examination of Figure 1 (and of the original plate) does not show any sodium line. However, when the flame was viewed with a pocket spectroscope the sodium D lines were observed. They were weak and fleeting, indicating the presence of sodium only in traces. This leads to the conclusion that the characteristic yellowish color of the acid-aniline flame is due almost entirely to the spectral distribution of radiation from incandescent carbon particles at about 2700°K.

The densities of the flame spectra and of the known tungsten spectra were compared at 13 points at intervals of 200A between 3600A and 6000A. The resulting intensity curve for the flame spectrum is shown in Figure 2. The very weak band systems, which were barely perceptible on the densitometer traces, are not indicated on Figure 2. The ordinates of Figure 2 are ergs/cm² sec per 2π steradians.

To obtain the temperature and the emissivity from Figure 2, Wien's equation for the spectral distribution of energy was chosen since it is accurate to 1 percent when

$$\lambda T < 0.3 \text{ cm degrees,}$$

a condition which is met throughout the spectral interval of Figure 2.

$$J_{\lambda} = \epsilon_{\lambda} C_1 \lambda^{-5} e^{-C_2/\lambda T} \quad (1)$$

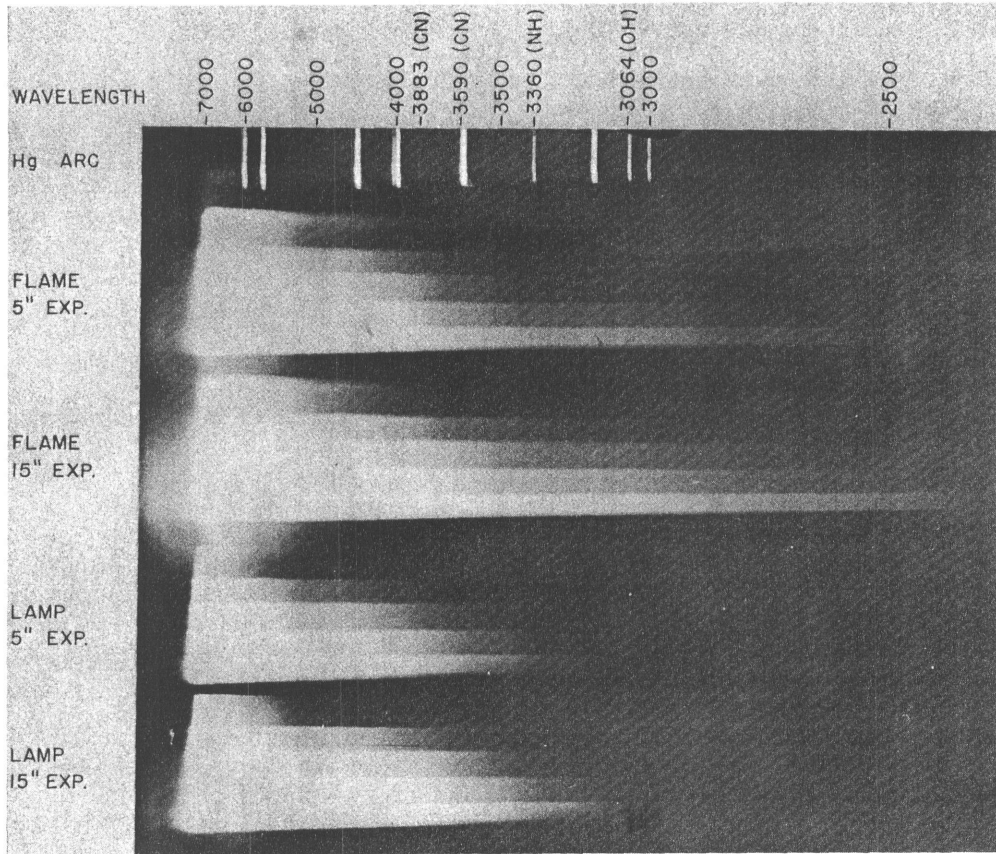


Fig. 1 - Comparison of Nitric Acid-Aniline Flame Spectra with Tungsten Spectra

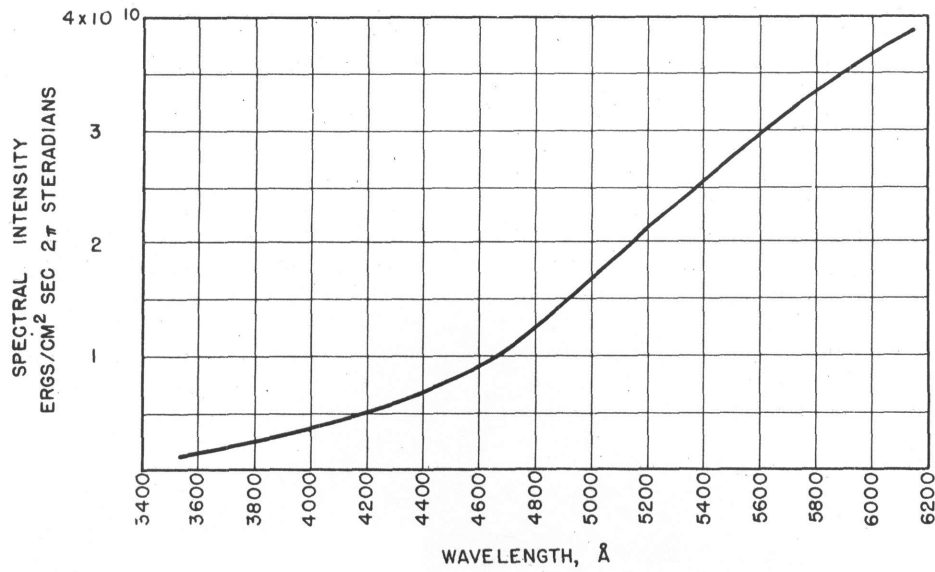


Fig. 2 - Spectral Intensity of Acid-Aniline Flame

where:

J_λ = spectral radiant intensity

ϵ_λ = spectral emissivity

C_1 = first radiation constant

= 1.177×10^{-12} watts cm^2

λ = wavelength in cm

C_2 = second radiation constant

= 1.432 cm degrees, and

T = temperature in degrees K.

Transferring λ^{-5} to the left hand side, and taking logarithms, to base 10,

$$\log (J_\lambda \lambda^5) = \log (\epsilon_\lambda C_1) - \frac{0.6219}{T} \frac{1}{\lambda} \quad (2)$$

Since $\log (\epsilon_\lambda C_1)$ is constant, or nearly so, since ϵ varies little with λ , Equation (2) represents a straight line, of slope $-0.6219/T$, between the variables $\log (J_\lambda \lambda^5)$ and $1/\lambda$.

Figure 3 is a graph of Equation (2) using values of J_λ from Figure 2. The slope of the curve is -2.29×10^{-4} , whence

$$T = \frac{0.6219}{2.29 \times 10^{-4}} = 2712^\circ \text{K.}$$

Returning to Figure 3, it is seen that the points fit a straight line rather well which is the justification for the statement above that $\log (\epsilon_\lambda C_1)$ is constant, or nearly so.

1000-Pound-Thrust Alcohol-Oxygen Flame

The spectrum was discontinuous between 2350A and 7000A, consisting of sharp lines and bands superposed on a relatively weak continuum. The spectrum is shown in Figure 4 in which the following lines and band systems are identified:

- Na - 5893A
- CaO - 5560 and 6260A
- OH - 2811 and 3064A
- CH - 4312A
- CO - continuum from 2350 to 5000A

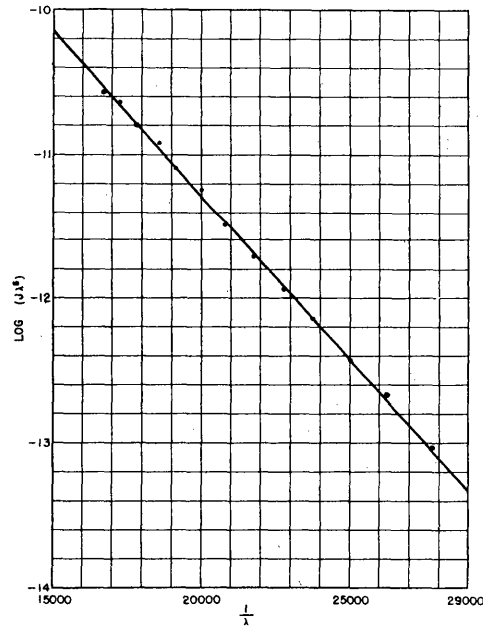


Fig. 3 - $\text{Log } (J_\lambda^5)$ vs $1/\lambda$

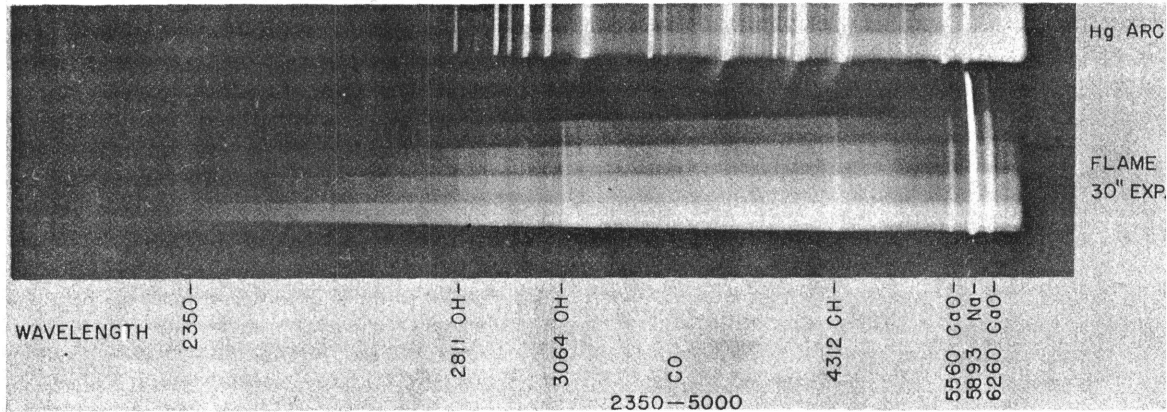


Fig. 4 - Spectra of Alcohol-Oxygen Flame

The plate was not calibrated with the tungsten lamp; hence, the true spectral distribution was not obtained.

On the occasion of these measurements, the supply of alcohol was used up before there was an opportunity to make total radiation intensity measurements. It can be said that observation indicates that the alcohol-oxygen flame is a less powerful emitter than the acid-aniline flame.

TOTAL RADIATION INTENSITIES

400-Pound-Thrust Motors

The intensity of the total radiation emitted by 400-pound-thrust acid-aniline motors was measured with a total radiation pyrometer comprised of a copper-constantan radiation thermocouple at the focus of a 4.5-cm-diameter, 3.5-cm focal length concave mirror, and a General Motors amplifier with 10-ma output meter to record thermocouple voltages. A Cassegrain eye-piece looking through a hole in the center of the pyrometer mirror gave a view of the flame image on the thermocouple, which permitted accurate aiming at the flame. The field of view of the thermocouple was $1^{\circ}26'$ by 2° . The instrument was hand-held and sighted on the flame at a distance of about 6 feet, so that the thermocouple viewed a rectangular section of the flame about 1.8 by 2.1 inches. Since the flames were about 9 inches in diameter and 6 or 7 feet long for 400-pound-thrust motors, the flame image was at all times larger than the thermocouple.

The pyrometer was calibrated with the radiation from two blackened rectangular cans filled respectively with cold and hot water at known temperatures and, hence, of known radiant intensities. By means of the calibration, thermocouple voltage registered when the pyrometer was aimed at the rocket flame could be interpreted as radiant intensity of the flame or, by means of the Stefan-Boltzman law, as equivalent blackbody temperature of the flame.

Two measurements were made on two separate runs of a 400-pound-thrust acid-aniline motor. It was chosen to aim the pyrometer at the most intense part of the flame about 2 feet from the jet orifice and outside the region nearer the orifice where the shock bands appeared. These results were obtained. On run 1, the equivalent blackbody temperature

of the flame was 980°K. Substitution of this number in the Stefan-Boltzman equation gave the result for radiant intensity

$$I = 1560 \text{ watts/ft}^2 \text{ steradian.}$$

On run 2, the equivalent blackbody temperature was 1015°K. The radiant intensity was

$$I = 1800 \text{ watts/ft}^2 \text{ steradian.}$$

Resume of Radiation Measurements

Results obtained by this Laboratory in the present work and in the earlier investigation are given in Table 1. The data for 220-pound-thrust motors were obtained in the earlier experiments described in Footnote 1. The measurements were made on the brightest part of the flames, and in each case the flame was viewed at a right angle to its length. The fourth column giving the steradiancy of the flames was obtained by substituting the measured equivalent blackbody temperature in the Stefan-Boltzman equation,

$$I = \frac{930\sigma T^4}{\pi} \tag{3}$$

where I = radiant intensity per square foot per steradian

$$\sigma = 5.73 \times 10^{-12} \text{ watts/cm}^2 \text{ deg}^4 \text{ per } 2\pi \text{ steradians}$$

T = temperature in degrees Kelvin,

and the factor 930 is the number of square centimeters per square foot.

The same equation was multiplied by the emissivity of the flame when the true flame temperature determined from the spectrum was used in the fourth and seventh lines of the Table.

TABLE 1

Radiant Intensities of Acid-Aniline Flames Measured at Reaction Motors by NRL

Motor Thrust (lb)	Equivalent blackbody temperature (°K)	Radiant intensity (watts/ft ² sterad)	Approximate flame area (ft ²)	Total intensity (watts/sterad)
220	855	910	2.5	2275
220	860	930	2.5	2320
220	780	630	2.5	1570
220		590*	2.5	1470
400	980	1560	5	7800
400	1015	1800	5	9000
400		505**	5	2525

* Based on Spectroscopic true temperature (2760°K), emissivity = 0.006.

** Based on spectroscopic true temperature (2712°K), emissivity = 0.0055.

Table 1 shows that in all cases the radiant intensities determined by direct measurement were larger than those computed from true temperature and the emissivity of the flame in the visible spectrum. The two kinds of result were more nearly alike for the 220-pound than for the 400-pound motors. A number of factors may have contributed to the variety of the results obtained, although each individual measurement is thought to be correct.

- a. The spectra and the total radiation measurements were obtained during different runs of the motors in all cases.
- b. It is thought that the values of emissivity in the visible spectrum of 0.006 and 0.0055 obtained for two flames were largely due to incandescent carbon particles in the flames. It is probable that the emissivity was higher in the infrared spectrum. If so, this higher emissivity was probably due to the CO₂ and H₂O emission bands which produced measured values larger than the computed values of total emission.
- c. While it is true that approximately the same values of temperature and emissivity were obtained for a 220-pound and a 400-pound motor, this fact indicates marked differences between the radiation characteristics of the two flames photographed. The intensity of the total radiation emerging from an emitting and absorbing flame is given by

$$E_f = E (1 - e^{-\alpha t}) \quad (4)$$

where E_f = total emission of the flame

E = total emission of a blackbody at the temperature of the flame

α = absorption coefficient of the flame (cm⁻¹)

t = flame thickness in cm.

Since t was greater in the 400-pound flames, the observed intensity of radiation should have been greater than that of the 220-pound flame. This was true of total radiation measurements but not of the spectroscopic measurements.

The results of Table 1 are thought to be individually correct. They form an adequate basis for estimation of infrared detection ranges of acid-aniline rocket missiles since they establish approximately the spectral distribution curve of the radiation and provide a number of values of total radiation emitted. Such estimates of detection range will be made in a later section of the report.

Aerojet Results

The spectral intensities in the infrared and the total radiation intensities of a number of large acid-aniline and other jet motor flames have been measured by the Aerojet Engineering Corporation.² Certain of the Aerojet data³ giving observed flux densities of total radiation at a distance of 100 feet and estimated flame area were used to compute the total radiant intensities.

² C. M. Wolfe, "Final Report on Contract NOa(s)-8472," Aerojet Eng. Corp., Report No. R-82, 30 Sept. 1947.

³ Ibid, Table 68.

The results are shown in Table 2. The equivalent black body temperatures shown in column 2 do not agree with those calculated by Aerojet. They were obtained by solving for T in the equation

$$F = \frac{A\sigma(T^4 - T_0^4)}{\pi R^2} \quad (5)$$

where F = observed flux density in watts/cm²

A = projected area of the flame as given by Aerojet

R = distance in cm at which F was measured

T = equivalent black body temperature of the flame

σ = the Stefan-Boltzman constant.

The equation used for this computation in the Aerojet report was:

$$4\pi R^2 F = \pi A\sigma(T^4 - T_0^4) \quad (6)$$

However, the right hand side of Equation (6) does not give total radiation over a sphere from a conical flame surface. The error in Equation (6) amounts only to a factor π/4, and the equivalent blackbody temperatures given in Table 2 do not differ greatly from those given in footnote 3. The difficult environment with which the experimentalist must contend at rocket test stands is likely to produce even larger experimental discrepancies in the best-planned measurements.

TABLE 2

Radiant Intensities of Acid-Aniline Flames Measured by Aerojet

Motor Thrust (lb)	Observed flux density at 100 ft (watts/cm ²)	Flame Dimensions		Projected Area (ft ²)	Equivalent blackbody temperature (°K)	Radiant Intensity watts/ft ² sterad	Radiant Intensity watts/sterad
		Length (ft)	Diam. (ft)				
1000 rich mixture	End View 3.4 x 10 ⁻³	10	2	3.14	1560	10400	32700
	Side View 8 x 10 ⁻³			10	1450	7400	74000
1100 lean mixture	3.4 x 10 ⁻³	10.8	2.2	11.3	650	300	3390
4000 lean mixture	7.8 x 10 ⁻³	24	4.8	55.7	940	1330	74000

It is to be noted that the radiation temperatures recorded in Table 2 take values both lower and higher than any in Table 1, the higher values applying to rich fuel mixtures and the lower values to lean fuel mixtures. This result does not mean necessarily that the true temperatures of the flames were different. They may have been different, but the higher emissivity of the rich, smoky flame may also have contributed to larger total emission and, hence, to larger computed values of equivalent blackbody temperature.

In the same way, a deeper layer of flame contributed to the observed high intensity in the end view of the flame, first line of Table 2, than in the side view. Hence, there is no inconsistency in the data of the first two lines of the table.

The motors described in Table 2 were larger than those described in Table 1, and the flames were of larger cross-sectional area. In no case is the effective radiating area accurately known. The estimated areas given in Tables 1 and 2 together with measured values of steradiancy lead to 1570 watts/steradian for a 220-pound motor as the smallest total emission of radiation that has been observed, and to 74,000 watts/steradian for the 1000-pound rich mixture and 4000-pound lean mixture as the largest value.

ON THE DETECTION OF ACID-ANILINE ROCKETS BY LEAD SULFIDE CELLS

The problem of estimating instrumentation for detection or measurement of rockets in flight requires evaluation of the integral

$$E = \int_{\lambda_1}^{\lambda_2} J_{\lambda} S_{\lambda} t_{\lambda} d\lambda \quad (7)$$

where E = total usable energy radiated in the spectral band
 λ_1 to λ_2 ,

J_{λ} = spectral emission by the flame,

S_{λ} = spectral sensitivity of the sensitive element, and

t_{λ} = spectral transmission of the atmosphere.

Numerical values for the three parameters are known with sufficient accuracy to permit evaluation of Equation (7) for certain cases.

Atmospheric Transmission

Figure 5 shows measured transmission coefficients of haze-free air containing known amounts of water vapor. The upper curve (a) was obtained by Fowle⁴ using an absorbing path length of 117 meters containing 0.082 cm of precipitable water. Fowle's curve has been shifted slightly to longer wavelengths in order to bring the water bands into their proper spectral positions. The dotted portion of Fowle's curve was drawn by guess except for the minima of the ρ band (0.92μ) and the ϕ band (1.1μ) which were calculated using the square root law from other data of Fowle's given by Fischer.⁵

⁴ F. E. Fowle, Water vapor transparency to low-temperature radiation, Smithsonian Misc. Collections 68, No. 8 (Oct. 27, 1917).

⁵ Heinz Fischer, On the absorption of water vapor in the infrared as a function of water path, US Air Force Technical Report 5660, Wright Field (21 Jan. 1948).

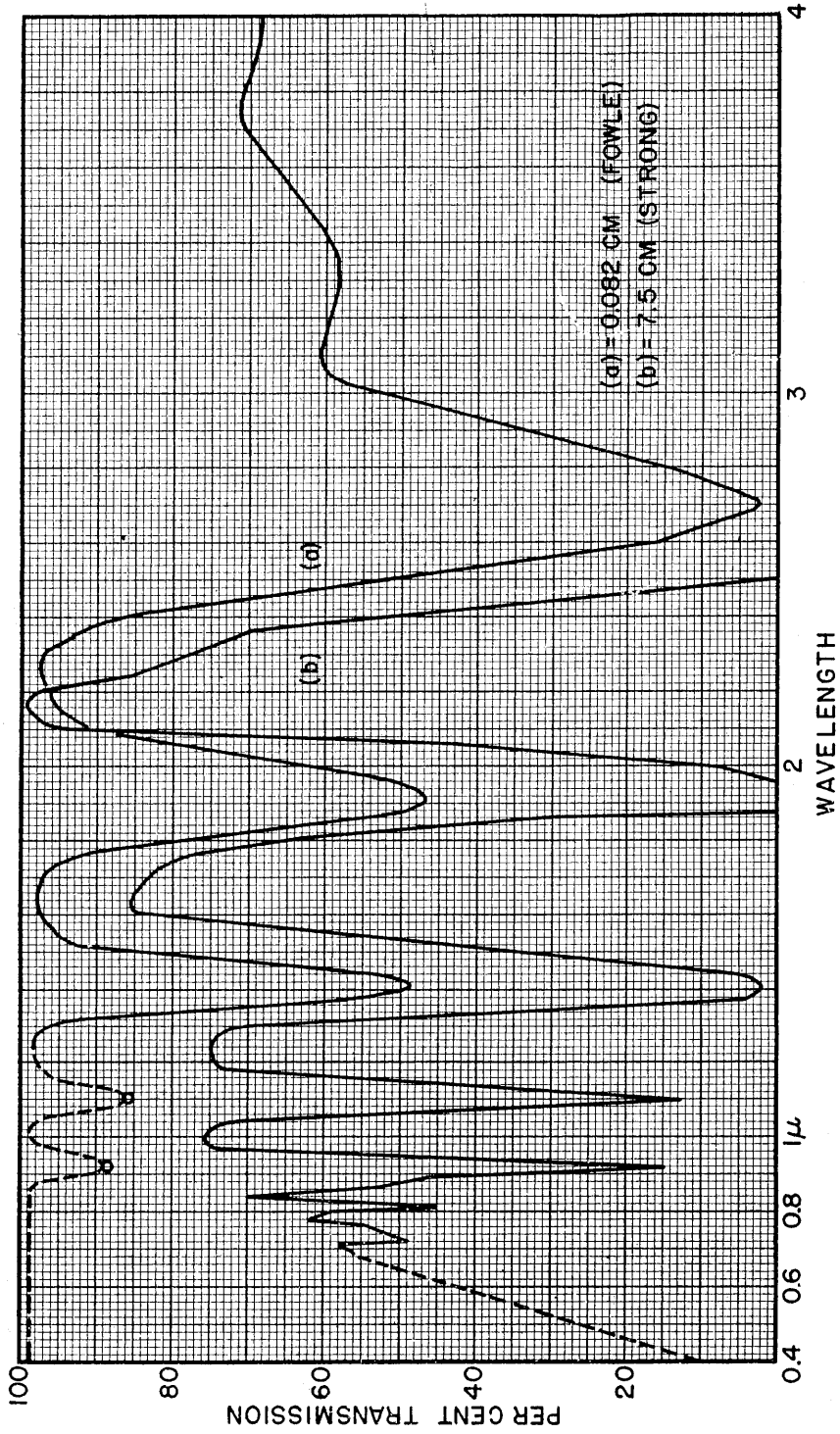


Fig. 5 - Spectral Transmission of 0.082 and 7.5 cm Precipitable Water Vapor

The lower curve (b) was obtained by Strong⁶ through 5000 yards of haze-free atmosphere containing 7.5 cm of precipitable water. The dotted portion of Strong's curve was drawn in by guess based on known absorption coefficients at 0.4μ and 0.7μ . This portion of the curve is in a spectral region which probably would be excluded by filters in a practical military application because it is a region of high solar intensity. It was thought that a more laborious estimate of the 0.4μ to 0.7μ region would not improve the value of this inherently inexact calculation.

The Spectral Intensity Viewed Through 0.082 and 7.5 cm of Water Vapor

The curves of Figure 5 may be used to estimate the nature of the acid-aniline flame spectrum viewed through the atmospheres represented by these curves. Figure 6 repeats Fowle's transmission curve for 0.082 cm of water (curve (a)) and shows the spectral intensity of a blackbody source at 2800°K (dotted curve (b)). The product $t_\lambda J_\lambda$ is shown in curve (c). It will be assumed that curve (c) represents closely enough the spectral intensity of an acid-aniline flame viewed through a path of any length containing a total of 0.082 cm precipitable water. Since the optical paths of interest will of necessity be at high altitude if so little water is to exist in a long path of military interest, attenuation by haze is conveniently neglected. Lack of knowledge of the pressure dependence of absorption may lead to errors in computations for high altitudes.

The choice of 2800°K as a blackbody temperature representative of acid-aniline flames was based on spectroscopic measurements in the ultraviolet and in visible spectra described earlier in the report. It was thought that the value 2800°K was equally as good as the values 2712°K and 2760°K obtained from spectra. Treatment of the flame as a blackbody of this temperature is supported by comparison of curve (c) of Figure 6 representing the calculated spectral distribution of energy through 0.082 cm water with infrared emission spectra observed by Aerojet.⁷ This has been done in Figure 7. Two sets of Aerojet data are shown with a single, dotted curve through them. Intensities were arbitrarily made equal to unity at 1μ , and the experimental points were translated toward shorter wavelengths by approximately 0.1μ to bring the minima, considered to be due to water-vapor absorption, into correct spectral positions. The Aerojet data were obtained through 115 feet of air which if saturated at 30°C , an ambient temperature recorded in footnote 2, would contain about 0.10 cm precipitable water. Hence, the water paths which apply to the calculated and the observed spectra of Figure 7 are approximately equal.

Either spectrum could be used in estimating the detection range of acid-aniline flames. The 2800°K blackbody spectrum is easy to deal with, and it will be used in subsequent calculations.

Figure 8 represents the product $t_\lambda J_\lambda$ for 7.5 cm of water and a 2800°K blackbody source using the transmission curve of Strong, Figure 5. Points at 3.4 and 4μ were estimated from other data. They were introduced to indicate that the available energy from this source at wavelengths above 3μ is small after traversal of 7.5 cm of water.

Integrated Transmission Coefficients

The integrated transmission coefficients

$$t = \frac{\int_{0.4}^{4.0} t_\lambda J_\lambda d\lambda}{\int_{0.4}^{4.0} J_\lambda d\lambda} \quad (8)$$

⁶ John Strong, Atmospheric attenuation of infrared radiations, OSRD Report 5986 (Nov. 30, 1945) Figure 14b.

⁷ C. M. Wolfe, Op. cit.

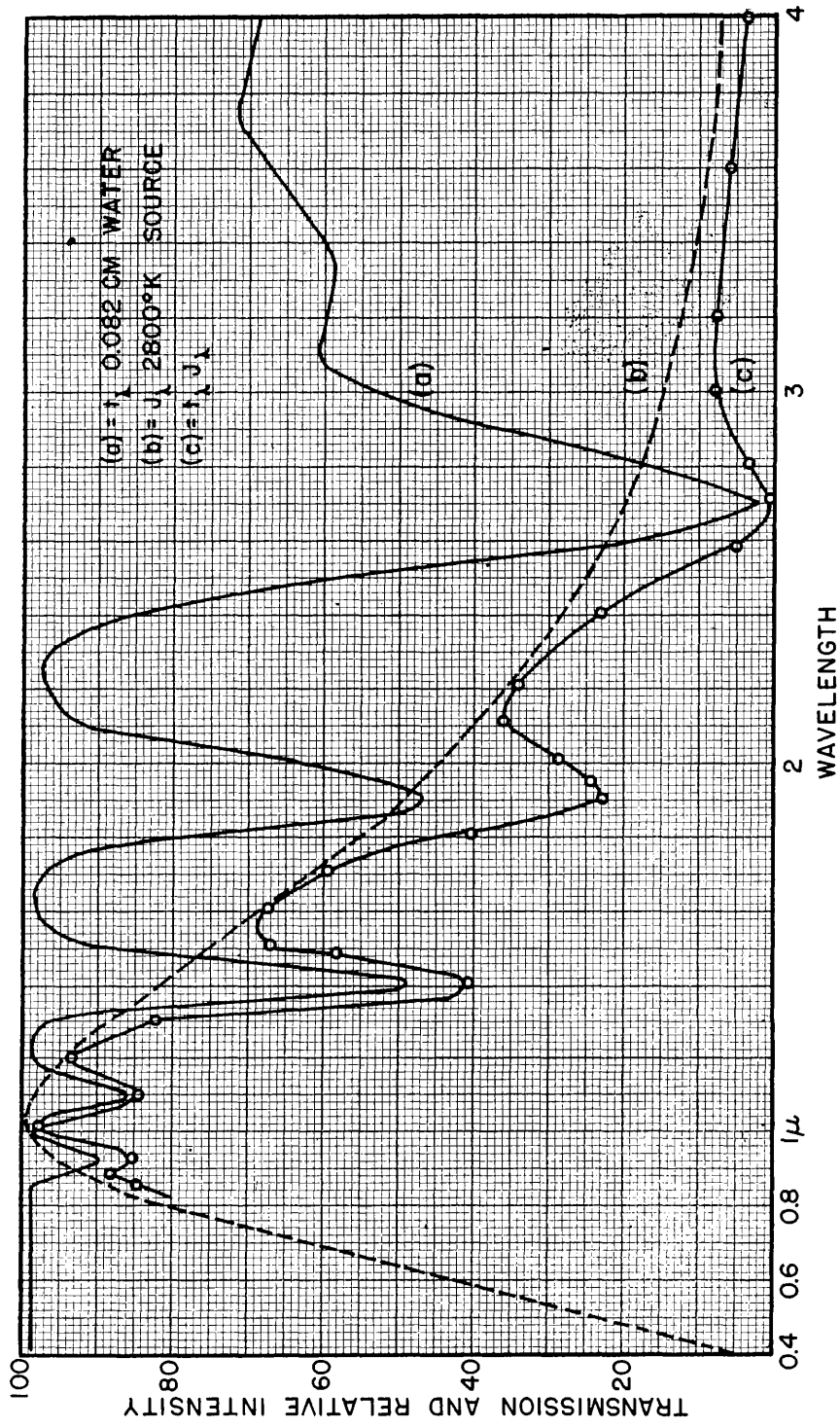


Fig. 6 - Product: Spectral Intensity of 2800°K Source and Transmission of 0.082 cm Water Vapor

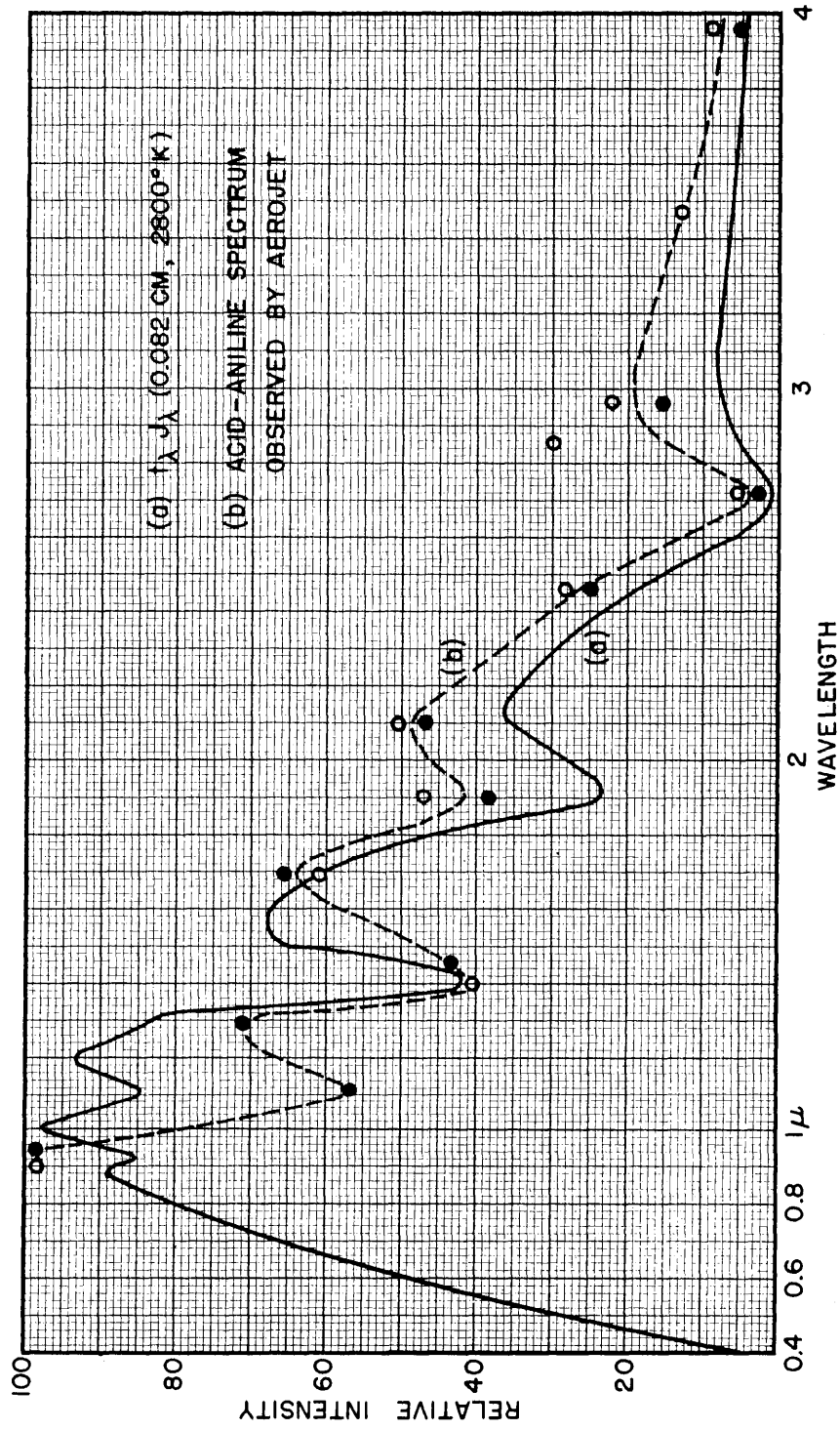


Fig. 7 - Comparison of 2800°K Source with Aerojet Flame Spectra

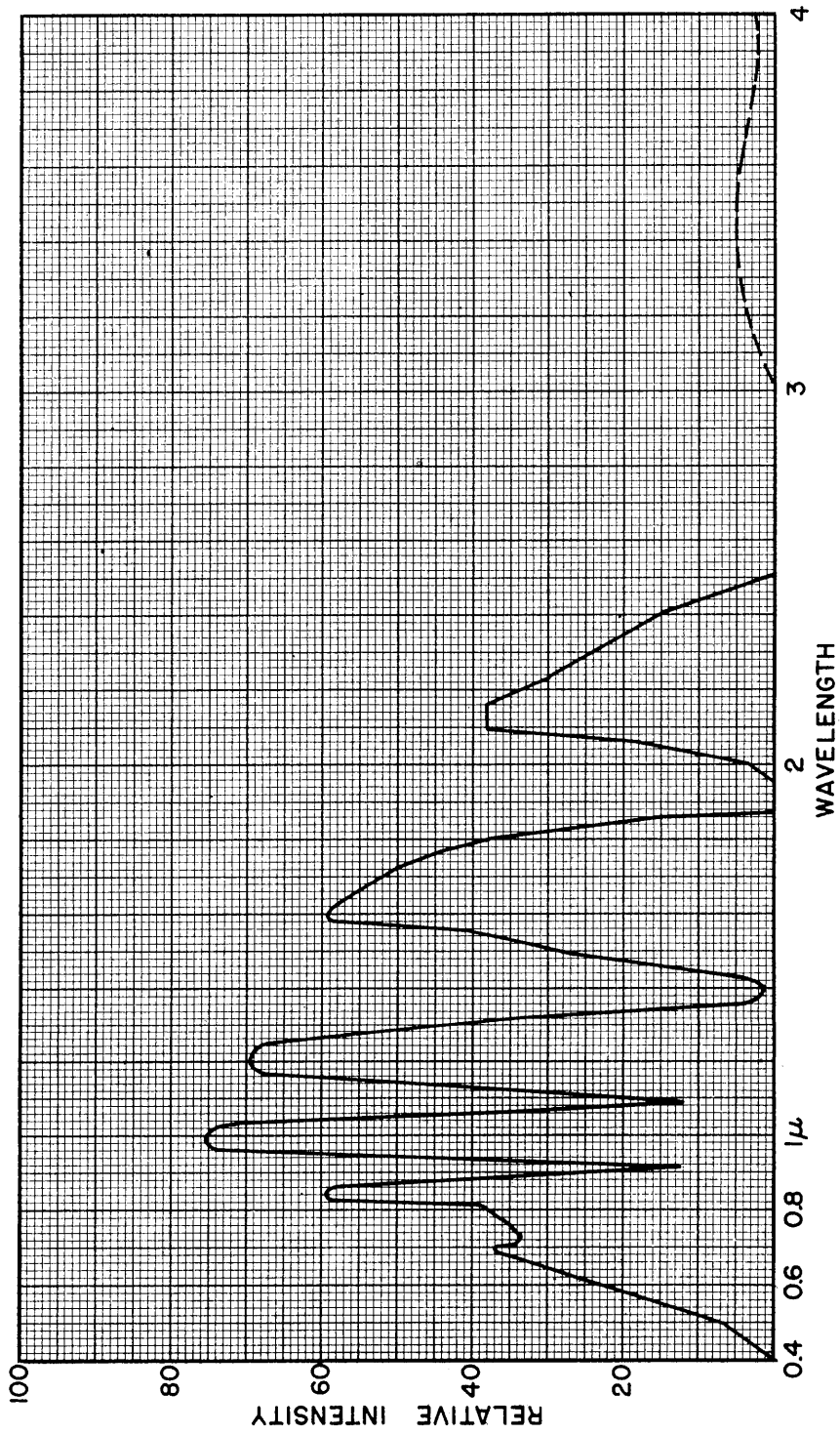


Fig. 8 - Product: Spectral Intensity of 2800°K Source
and Transmission of 7.5 cm Water Vapor

was computed from the ratio of the measured area under curve (c) to the area under curve (b) of Figure 6 for 0.082 cm water. The result was

$$t = 0.80$$

In the same way, the integrated transmission of 7.5 cm of water for 2800° K radiation was computed to be

$$t = 0.44$$

The dotted portion of the curve between 3 and 4 μ , Figure 8, contributed only 2 percent to this result and can well be neglected in further computations.

Sensitive Element

It is assumed that a lead sulfide cell would be used in detecting rocket flames. At the present time marked differences in spectral response are found among lead sulfide cells. Two spectral response curves have been chosen for use in this illustrative calculation: (a) the German Elac, chemically deposited cooled cell, and (b) a Cetron uncooled cell prepared by sublimation of the lead sulfide. They are given in Figure 9. The Elac cell was measured by Oxley;⁸ the Cetron cell was recently measured by the National Bureau of Standards and reported informally. These two response curves represent extremes, the peak sensitivity of the Cetron cell being at 0.7 μ and that of the Elac cell being at 2.5 μ .

The lead sulfide cell of long-wavelength sensitivity with peak at 2.5 or 2.7 μ is the more desirable type for general application. It is said that Admiralty Research Laboratory cells peak at 2.7 μ . Cashman cells exhibit peak sensitivity at wavelengths 2 to 2.8 μ .⁹ It appears certain that the type of spectral response illustrated by the Elac curve, Figure 9, will eventually become standard. It was instructive, however, to make the calculations for this specialized application to the detection of rocket flames for both types of cells illustrated by Figure 9. The Cetron and Elac cells were chosen for the purpose of the calculation because more complete data were available for them than for any others. In particular, the spectral response curves were known both in the visible and in the infrared spectra which was of convenience when used in connection with a 2800° K target temperature.

Figure 10 shows the product $t_{\lambda} J_{\lambda} S_{\lambda}$ for each of these cells, an atmosphere containing 0.082 cm of water and a 2800° K blackbody source. The ratio of the area under the Cetron curve to the area under the Elac curve is 0.80, showing that, on the basis of spectral response alone, there would be little difference in the effectiveness of the cells as detectors of acid-aniline flames through 0.082 cm of precipitable water. This comparison does not, of course, include the absolute sensitivities of the cells. Such a comparison will be made later in the report.

The integrated atmospheric transmission factors of 0.082 cm of water vapor for the fractions of the total radiation from a 2800° K source detectable by the Cetron cell and the Elac cell were calculated by taking the ratios of the areas under the curves of Figure 10, respectively, to the integral

$$\int_{\lambda_1}^{\lambda_2} J_{\lambda} S_{\lambda} d\lambda$$

⁸ C. L. Oxley, "The Elac lead sulfide photocell," NRL Report H-2774 (18 July 1946).

⁹ R. J. Cashman, "Development of sensitive lead sulfide photo-conductive cells," OSRD 5998, Contractor's Report No. 64 on Contract OEMsr-235 (Oct. 31, 1945).

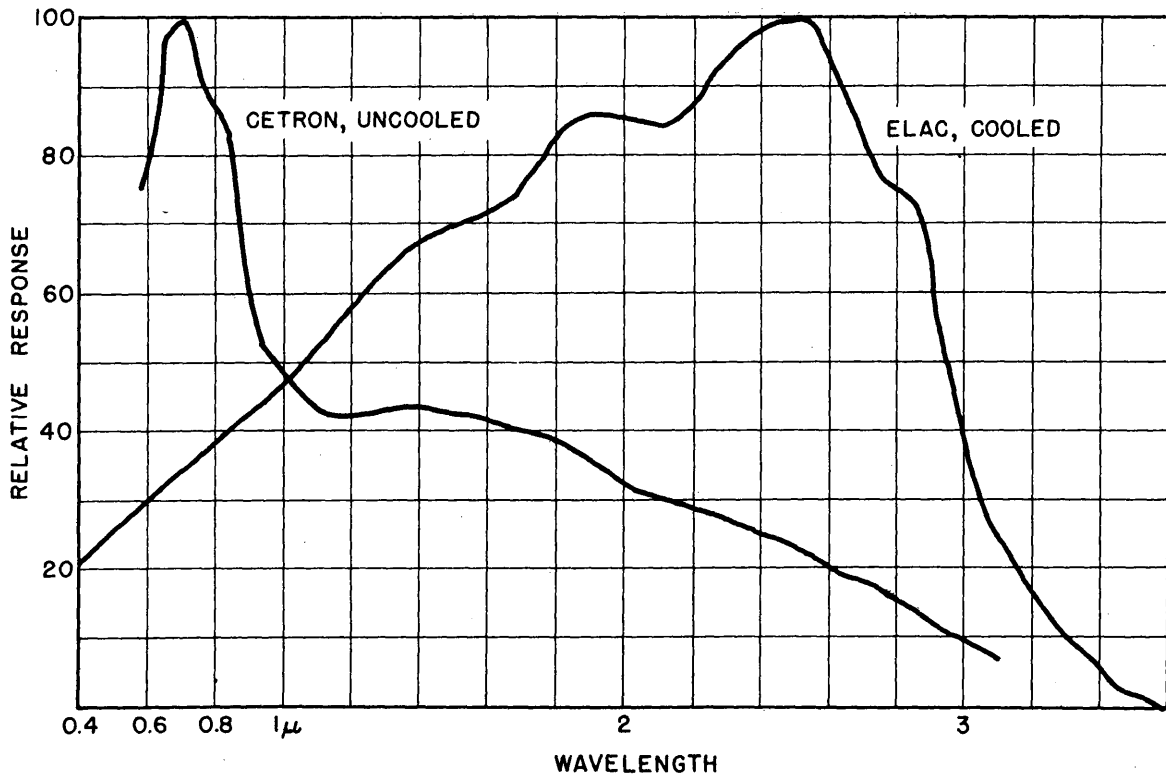


Fig. 9 - Spectral Response of Cetron and Elac Cells

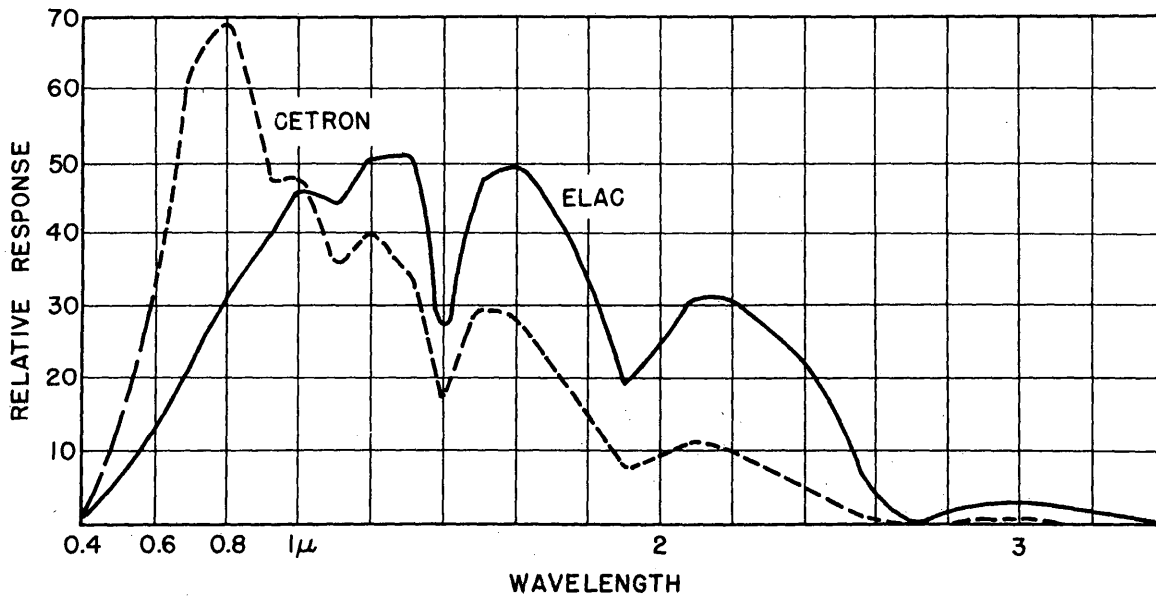


Fig. 10 - Product: $t_{\lambda}J_{\lambda}S_{\lambda}$ for 0.082 cm Water, 2800°K Source and Two PbS Cells

where λ_1 and λ_2 are the lower and upper wavelengths at which $J_\lambda S_\lambda = 0$. The product curve $J_\lambda S_\lambda$ for each cell is shown in Figure 11. The integrations were carried out between $\lambda_1 = 0.4\mu$ and $\lambda_2 = 3.2\mu$ for the Cetron cell, and $\lambda_1 = 0.4\mu$, $\lambda_2 = 3.6\mu$ for the Elac cell and, when divided into the corresponding areas under the curves of Figure 10, led to integrated atmospheric transmission coefficients

$$\begin{aligned} \text{Elac} \quad t_{0.082} &= 0.79 \\ \text{Cetron} \quad t_{0.082} &= 0.86. \end{aligned}$$

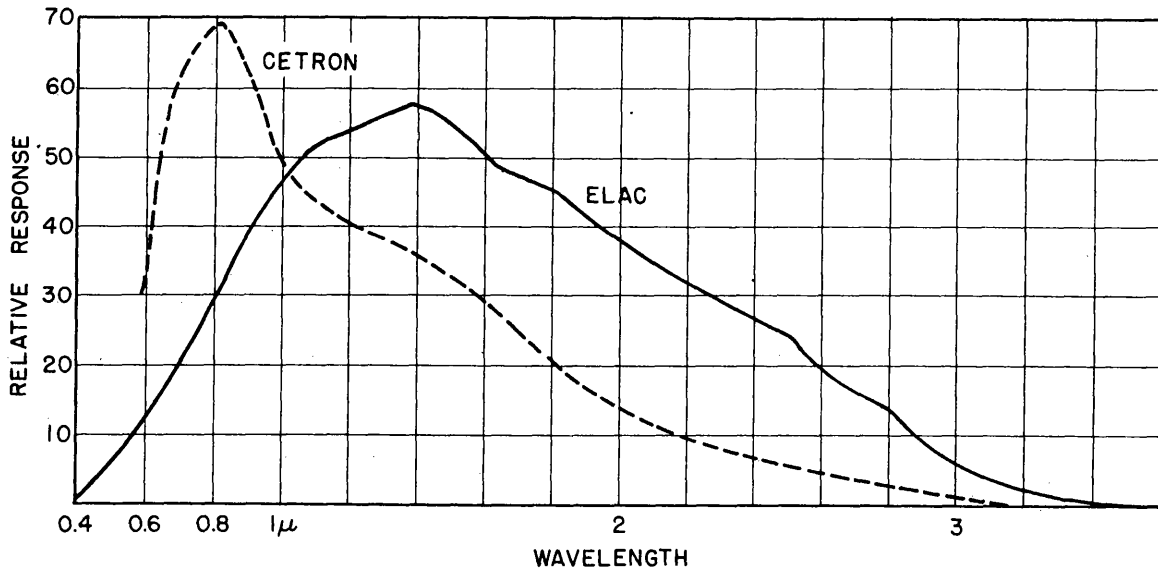


Fig. 11 - Product: Spectral Intensity of 2800° K Source and Two PbS Cells

The same calculations have been made for an atmosphere containing 7.5 cm of precipitable water. Figure 12 shows the products $t_\lambda J_\lambda S_\lambda$ for each cell. The integrated atmospheric transmission coefficients calculated as described above were

$$\begin{aligned} \text{Elac} \quad t_{7.5} &= 0.44 \\ \text{Cetron} \quad t_{7.5} &= 0.48. \end{aligned}$$

It is evident that the widely differing spectral response characteristics of the two cells do not, in this particular application, lead to any marked superiority of one cell.

There are no data on the response of the two cells to 2800° K radiation and the Elac cell is not available for measurement. However, the sensitivities of both cells for radiation from a blackbody source at approximately 800° C are on record, and the sensitivities in absolute units to 2800° K radiation can be deduced by the analytical procedures used above.

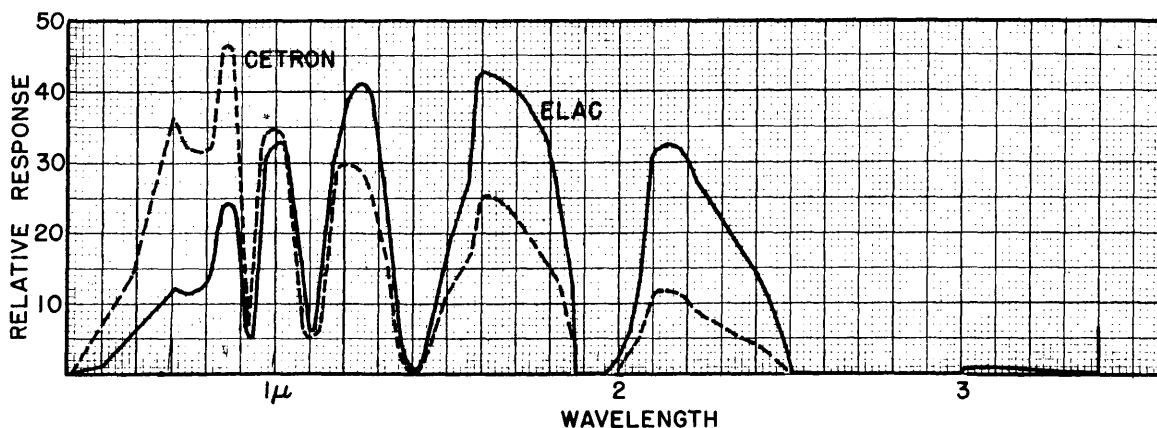


Fig. 12 - Product: $t_{\lambda} J_{\lambda} S_{\lambda}$ for 7.5 cm Water, 2800°K Source and Two PbS Cells

The Elac cell response to 1100°K radiation was measured by Harvey.¹⁰ The flux density of this radiation required to produce a signal equal to noise was 1.16×10^{-7} watts/cm² with an amplifier passing frequencies 6 to 700 cps. The radiation was modulated by a square wave chopper operating at 15 cps.

A comparison of the ratios $\int J_{\lambda} S_{\lambda} d\lambda / \sigma T^4$ for 2800°K and 1100°K sources showed that the Elac cell would utilize a fraction of 2800°K radiation about 1.86 times greater than the fraction of 1100°K radiation to which it was sensitive. Hence, with the same amplifier, the total radiation input from a 2800°K source which would produce a signal equal to noise should be

$$\text{ENI (Elac)} = 6.25 \times 10^{-8} \text{ watts/cm}^2.$$

The same computation employing characteristics of the Cetron cell showed that it should be 4.3 times more sensitive to 2800°K radiation than to 1100°K radiation. The measured ENI for 1100°K radiation was 3.6×10^{-7} watts/cm² with amplifier bandwidth of 6 to 60,000 cps. Hence, for 2800°K radiation,

$$\text{ENI (Cetron)} = 8.4 \times 10^{-8} \text{ watts/cm}^2.$$

The wider bandwidth with which the Cetron cell was used should have produced $(60000/694)^{1/2} = 9.3$ times greater noise than the 6 to 700 cps amplifier of the Elac measurements. It will be assumed that both cells would be used with amplifiers of about 3000 cps bandwidth, which would be appropriate in the KIEL IV, for example.¹¹ The equivalent noise

¹⁰ G. L. Harvey, "Sensitivity of the Air to Air Infrared Kiel IV," NRL Letter Report C-600-365/47 (Dec. 1947).

¹¹ R. J. Cashman, Op. cit.

inputs of the two cells for 2800°K radiation, 3000 cps bandwidth should be

$$\text{ENI (Elac)} = 1.3 \times 10^{-7} \text{ watts/cm}^2$$

$$\text{ENI (Cetron)} = 1.84 \times 10^{-8} \text{ watts/cm}^2.$$

These values apply when the cells are in a uniform field of 2800°K radiation covering the entire sensitive areas of the cells. In order to compute the signal-equal-to-noise produced by the focussed image of a military target it is necessary to assume uniform sensitivity over the sensitive area of the cell, a condition which is rarely found in present lead sulfide cells. Then the focussed radiation signal, equal to noise, is given by multiplying the numbers above by the sensitive areas of the cells, 0.09 cm² in the case of the Elac cell and 0.48 cm² for the Cetron cell. Hence, the signals equal to noise should be

$$\text{EN (Elac)} = 1.2 \times 10^{-8} \text{ watts}$$

$$\text{EN (Cetron)} = 0.9 \times 10^{-8} \text{ watts.}$$

Therefore, there appears to be little difference in sensitivity of the two photocells as detectors of the radiation from acid-aniline flames.

In practice, cells having highest sensitivity in the 2 to 2.7μ region would be chosen for the sake of increased sensitivity to cooler targets which may not emit flames.

Detection of Acid-Aniline Flames

The foregoing data permit estimates to be made of the detectability of acid-aniline flames by lead sulfide cells in specific cases. The following conditions are chosen. Let the optical system be 30 cm in diameter and 30 cm in focal length. At useful ranges, the optical system will form an image of the flame smaller than the sensitive area of the lead sulfide cell. It is assumed that the radiation characteristics of the rocket in flight are those which have been measured on test stands. The computation will be made for detection at night in the absence of disturbing background radiation.

Under these conditions, the signal-to-noise ratios can be computed for atmospheres containing no haze and total amounts of water of 0.082 and 7.5 cm, for which integrated transmission coefficients have been obtained above. It is convenient to use the NACA Standard Atmosphere¹² which defines the pressure and temperature of the atmosphere an altitude of 50,000 feet, beginning with air temperature 15°C at sea level. It will be assumed in all cases that the atmosphere is saturated with water vapor. These conditions lead to the results of Table 3, which show the temperature, the relative partial pressure of water vapor, and the horizontal ranges in sea miles containing 0.082 and 7.5 cm of precipitable water, - all as function of altitude. The fact that points along the optical path between target and detector are not at constant altitude but lie along a chord through the atmosphere has been neglected. Computation of the complex atmosphere through which the detector would view the target would not increase the certainty of the final results of these calculations, and it has not been attempted.

The signal-to-noise ratio produced by a rocket flame in a system containing either of the lead sulfide cells described above at the focus of a 30-cm-diameter mirror is given by

$$S/N = \frac{IAwt}{(ENI)} = \frac{IAta}{R^2 \times 10^{-6}} \quad (9)$$

¹² See Smithsonian Physical Tables, p. 559 (8th revised ed.).

TABLE 3
Properties of the Atmosphere

Altitude (ft)	Temperature (°C)	e/e_0	Range Containing 0.082 cm water	Range Containing 7.5 cm water
0	15	1.0	71 yards	3.2 sea miles
10000	-4.8	0.24	296 yards	13.3 sea miles
20000	-24.6	0.035	1 sea mile	91.4 sea miles
30000	-44.4	0.004	8.8 sea miles	
40000 to 50000	-55.0	0.0014	25 sea miles	

where

I = steradiancy of the rocket flame, in watts/ft²
steradian,

A = cross sectional area of the flame in square feet,

w = solid angle subtended at the rocket by the optical
system = a/R^2 ,

a = area of the mirror, in cm²,

R = target range in cm,

t = integrated transmission coefficient for the
particular atmosphere and lead sulfide cell
under consideration, and

(ENI) = equivalent noise input of the cell = 10^{-8} watts.

Equation (9) has been evaluated for certain specific cases. The values of I and A were from Tables 1 and 2. The transmission coefficients, t , were those for 0.082 and 7.5 cm of water, obtained in an earlier section of this report. The area, a , was taken as 700 cm² (30-cm-diameter optical system) and R , the horizontal range, in cm containing 0.082 and 7.5 cm of water at selected altitudes.

The results are given in Table 4. From the first line of the table, a 220-pound-thrust motor of steradiancy 910 watts/ft², area 2.5 ft² viewed at 10,000 feet through 13.3 miles of atmosphere containing 7.5 cm of precipitable water should produce a signal-to-noise ratio of 12, etc. These results apply only to detection at night in the absence of disturbing background radiation. Furthermore, it must be assumed that a large signal-to-noise ratio of 50 or 100 will be required to assure positive operation of a pilotless missile or aircraft, although a detection or tracking system with ink recording or visual observation of oscilloscope traces may operate at a lower signal-to-noise ratio. Thus, it is possible that the flame of the 220-pound motor would be detectable at 25 sea miles at 40,000 feet altitude ($S/N = 6$), or at 13 sea miles at altitude 10,000 feet ($S/N = 12$). It is possible that a lead sulfide homing device would operate against this target at 9 sea miles, altitude 30,000 feet, $S/N = 50$.

TABLE 4

Estimated Signal-to-Noise Ratio in Lead Sulfide Detection System at Several Ranges Containing 0.082 and 7.5 cm of Water. Attenuation by Scattering Has Been Neglected

Acid-aniline motor (lb) thrust	Total intensity (watts/sterad)	Altitude (ft)	Range Containing 0.082 cm water (sea miles)	S/N	Range Containing 7.5 cm water (sea miles)	S/N
220	2275	10000	-----	--	13.3	12
		20000	1	4000	91.4	0.2
		30000	8.8	50	---	
		40000	25	6	---	
400	9000	10000	-----		13.3	50
		20000	1	16000	91.4	1
		30000	8.8	200	---	
		40000	25	25	---	
1000 (Side view - rich mixture)	74000	10000	-----	--	13.3	400
		20000	1	--	91.4	9
		30000	8.8	1600	---	
		40000	25	200	---	
1100 (lean mixture)	3390	10000	-----	--	13.3	19
		20000	1	--	91.4	0.4
		30000	8.8	77		
		40000	25	9		
4000 (lean mixture)	Same as 1000 lb. rich mixture					

A homing device would probably operate against the 1000-lb motor at 25 miles at altitude 40,000 feet, S/N = 200, or at 13 miles at 10,000 feet, S/N = 400, or it might be detectable at 91 miles at altitude 20,000 feet, S/N = 9.

The data and the methods which have been given will permit the reader to make similar estimates for particular situations. It must be remarked that the atmospheric transmission coefficients which have been used assume no attenuation by haze. Although the characteristics of 7.5 cm of water were based on a curve obtained by Strong under conditions described as "zero haze" as defined in his report, the measurements were made through a 5000-yard path at sea level where certainly the scattering by haze was greater than it would be at, say, 30,000 feet. The measurements of Fowle on 0.082 cm of water, on the other hand, were made through a path length of 71 yards in which attenuation by haze was unimportant.

It is not proposed to attempt corrections for the effect of haze on the calculated signal-to-noise ratios beyond the remark that at altitudes where haze and clouds exist detection ranges may be reduced virtually to zero.

In the case of haze-free dry air the attenuation of the signal by scattering by air molecules would further reduce the signal. Estimates of the transmission by 100 sea miles of dry air at 15°C and 760 mm pressure indicate transmission coefficients of 1.3 percent at 0.7 μ , 16 percent at 0.8 μ , 21 percent at 0.9 μ , 38 percent at 1.0 μ , 96 percent at 2 μ , and

99 percent at 3μ . These numbers were obtained from computed Rayleigh scattering coefficients in the range 0.7μ to 1μ where the index of refraction of dry air is known. Values of scattering coefficients at 2μ and 3μ were extrapolated from 1μ by the λ^{-4} relation assuming that the index of refraction was equal at 1μ , 2μ , and 3μ .

Clearly, at shorter wavelengths attenuation by scattering may be more pronounced than attenuation by water-vapor absorption. At longer wavelengths the attenuation by air scattering may be small. In any practical application the line of sight of a detection equipment would pass through a complex atmosphere, either along a chord or secant, and the attenuation both by water vapor absorption and scattering would be complex.

CONCLUSIONS

The computations which have been made lead to the conclusion that useful detection or homing ranges, in excess of 25 sea miles, may be obtained against acid-aniline rockets in flight at night. The computed signal strengths of Table 4 are sufficiently large to encourage airborne measurements against such rockets in flight, both at night and in daylight, in order to establish more definitely the detection and homing ranges to be expected with airborne equipment. The results of such airborne measurements would bring to the fore the effects of aircraft vibration, disturbance of the system by sunlight reflected from clouds, nonuniformity of the sky background, and other factors which must be known to permit the design and development of equipment having useful and achievable military characteristics.

* * *